*European Journal of Organic Chemistry*

EurJOC
European Journal of Organic Chemistry

Chemistry Europe
European Chemical Societies Publishing

RESEARCH ARTICLE OPEN ACCESS

# Diarylethene-Containing Photoswitchable Analogues of Tubulysins—Design, Synthesis, Biological, and Structural Evaluation

Anna Iampolska[1] | Sergii Afonin[2] | Oleg Babii[2] | Mahri Park[1] | Juan Estévez-Gallego[3] | Michel O. Steinmetz[3,4] | Andrea E. Prota[3] | Anne S. Ulrich[2,5] | David R. Spring[1] | Igor V. Komarov[6,7]

[1]Yusuf Hamied Department of Chemistry, University of Cambridge, Cambridge, UK | [2]Institute of Biological Interfaces (IBG-2), Karlsruhe Institute of Technology (KIT), Karlsruhe, Germany | [3]PSI Center for Life Sciences, Paul Scherrer Institut, Villigen, Switzerland | [4]Biozentrum, University of Basel, Basel, Switzerland | [5]Institute of Organic Chemistry (IOC), KIT, Karlsruhe, Germany | [6]Taras Shevchenko National University of Kyiv, Kyiv, Ukraine | [7]Lumobiotics, Karlsruhe, Germany

**Correspondence:** Anne S. Ulrich (anne.ulrich@kit.edu) | David R. Spring (spring@ch.cam.ac.uk) | Igor V. Komarov (igor.komarov@knu.ua)

**Received:** 19 May 2026 | **Revised:** 13 July 2026 | **Accepted:** 22 July 2026

**Keywords:** crystallography | diarylethene | medicinal chemistry | photopharmacology | photoswitchable peptidomimetics

## ABSTRACT

The discovery of tubulysins sparked considerable interest due to their high cytotoxic activity against multidrug resistant tumors. Total synthesis of these complex natural products—peptidic metabolites from myxobacteria *Archangium gephyra* and *Angiococcus disciformis*—demonstrated the power of organic chemistry and paved the way for the development of simpler, more stable, and selective derivatives. Despite these significant achievements, tubulysins are not used as stand-alone drugs due to their toxic side effects. In this study, we outline the design, synthesis, and evaluation of photoswitchable tubulysin analogues, which could be starting points for development of photopharmacological therapies aimed at addressing the toxicity challenges associated with tubulysins. The cytotoxic activity of one of the key analogues was shown to be light-controllable. For the first time, we provide a comparative analysis of the crystal structures of both photoisomers of a diarylethene-containing compound complexed with target proteins. This comparison enables a mechanistic explanation for the experimentally observed differences in the target binding efficiency and respective activity between the two photoisomers of the photoswitchable tubulysin analogue.

## 1 | Introduction

In recent years, the concept of using reversibly photoswitchable drugs, known as photopharmacology, has gained significant attention. Increasingly, scientific publications describe the development of photoswitchable bioactive compounds whose activity can be toggled by light irradiation. Light-controlled modulation was reported for antibiotics, enzymes, receptors, transport proteins, elements of the cytoskeleton, nucleic acids, lipids, and other biomolecules [1–4].

Utilizing photoswitchable drugs presents a promising strategy to mitigate systemic drug toxicity [3, 4]. In one scenario of their use, these drugs can be administered in less active and less toxic form, then activated—"switched on"—by light in the specifically targeted site/tissue/organ, thereby enhancing safety of the therapy. Another scenario, based on "switching off" a drug after treatment, is also an exciting distinctive feature of photopharmacology that might additionally alleviate problems caused by long-term circulation of a toxic drug. Recent in vivo studies have experimentally demonstrated potential safety advantages of photopharmacology over conventional drug treatments [5]. However, substantial work remains to be done in developing clinically useful photopharmacology therapies [6]. It is crucial, therefore, to continue exploring new photoswitchable biologically active compounds as candidates for photopharmacological treatments. This

paper presents our findings on the design, synthesis, biological evaluation, and structural analysis of photoswitchable analogues of the well-known cytostatic compounds, tubulysins.

Natural tubulysins were initially isolated from myxobacteria *Archangium gephyra* and *Angiococcus disciformis* and described by Reichenbach and colleagues in 2000 [7]. The chemical structures of some early-described members of the tubulysin family are shown in Figure 1a. These molecules are composed of four amino acid fragments: (*R*)-*N*-methylpipecolic acid (**Mep**), isoleucine (**Ile**), tubuvaline (**Tuv**), and tubuphenylalanine (**Tup**) or tubuphenyltyrosine (**Tut**). The **Tuv** residue is *N*-substituted by a group with a variable structure. Later studies have discovered many other members of this family [8], revealing significant diversity in their biosynthesis pathways [9]. It is interesting that tubulysins exhibit no activity against bacteria and yeasts, but demonstrate growth inhibition against filamentous fungi and extremely high cytotoxicity against eukaryotic cells [7–9]. Their mechanism of action is well-studied: they perturb microtubule dynamics in eukaryotic cells by binding to $\alpha\beta$-tubulin heterodimers, the building blocks of microtubules. This leads to the destabilization of the cytoskeleton, inhibiting cell division, cell cycle arrest and ultimately causing cell death through apoptosis [9, 10].

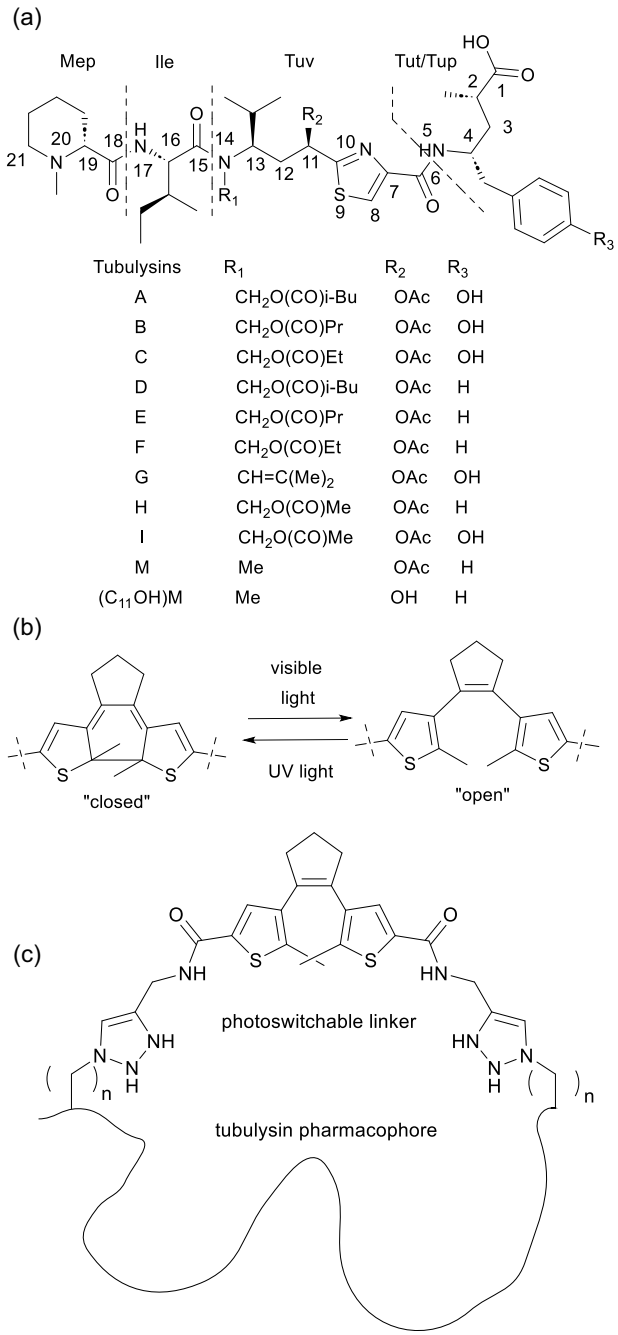


| Tubulysins | $R_1$ | $R_2$ | $R_3$ |
|---|---|---|---|
| A | $CH_2O(CO)i\text{-}Bu$ | OAc | OH |
| B | $CH_2O(CO)Pr$ | OAc | OH |
| C | $CH_2O(CO)Et$ | OAc | OH |
| D | $CH_2O(CO)i\text{-}Bu$ | OAc | H |
| E | $CH_2O(CO)Pr$ | OAc | H |
| F | $CH_2O(CO)Et$ | OAc | H |
| G | $CH{=}C(Me)_2$ | OAc | OH |
| H | $CH_2O(CO)Me$ | OAc | H |
| I | $CH_2O(CO)Me$ | OAc | OH |
| M | Me | OAc | H |
| $(C_{11}OH)M$ | Me | OH | H |

**FIGURE 1** | Prototype molecules, **DAE** fragment, and target photoswitchable analogues. (a) Some representatives of natural tubulysins. (b) Structure of the **DAE** moiety used for the tubulysin modification in this work, its photoconversion, and nomenclature of the photoisomers. (c) Schematic representation of the photoswitchable tubulysin analogues synthesized in this work with the **DAE** fragment shown in the open form.

Tubulysins hold great promise as lead compounds for developing anticancer drugs, with tubulysin D and M showing potent activity in the picomolar range against various cancer cell lines. However, due to significant systemic toxicity, they cannot be used as stand-alone drugs. Instead, they have found use in antibody-drug conjugates [11] and in small-molecule drug conjugates [12]. High potency combined with systemic toxicity prompted scientists to develop photoregulated cytotoxic agents based on tubulysins, aiming to alleviate the off-target toxicity issue. While the "photo-uncaging" approach to release active tubulysins via light irradiation has been known for more than a decade [13], reversibly photoswitchable tubulysin analogues remain undescribed. Such analogues could provide a basis for developing photopharmacology drugs and potentially avoid the drawbacks associated with the abovementioned photoactivatable/caged tubulysins, such as the formation of toxic byproducts upon irradiation and nonoptical drug release.

In this work, we designed tubulysin analogues containing a photoisomerizable diarylethene (**DAE**) fragment, a well-known bistable "molecular photoswitch" that has demonstrated effective performance in vivo and in vitro in photoswitchable antibiotics [14–17], enzyme inhibitors [18–23], protein–protein interaction disruptors [24], and cell-penetrating agents [25]. We hypothesized that the reversible photoconversion of the **DAE** moiety between ring-"open" and ring-"closed" forms (Figure 1b) can significantly alter the binding affinity of **DAE**-containing tubulysin analogues to the $\alpha\beta$-tubulin heterodimers. We were inspired by the works in which non-**DAE** photoisomerizable fragments have been successfully applied to obtain photocontrollable analogues of natural compounds, which perturb microtubule dynamics. These include taxanes (modified with azobenzene) [26], epothilones (styrylthiazole analogues) [27], and colchicinoids (modified by azobenzene [28–30], spiropyran [31], hemithioindigo [32], pyrrole hemithioindigo [33], and styrylbenzothiazole [34] fragments). These efforts led to the design and synthesis of numerous reversibly photoisomerizable small molecules, enabling efficient photocontrol of cytoskeleton-dependent processes both in vitro and in vivo. Despite these successes, the arsenal of actin dynamics modulators—specifically those based on peptides and peptidomimetics—remains sparse. A notable exception is the series of analogues of the F-actin-stabilizing depsipeptide jasplakinolide developed by Arndt and colleagues [35]. However, as with many of the examples mentioned above, although they demonstrate potent activity in vitro, the *Z*/*E*-type photoswitching often requires low-wavelength light irradiation.

This poses a risk of high phototoxicity, which hampers application of such molecules even in in vitro cell culture tests [36].

Our experience in designing **DAE**-containing photoswitchable peptide-based compounds [14–16, 21, 24, 25] and available literature data [37, 38] suggest that the target tubulysin analogues should be designed as macrocyclic molecules. Changes in the structure and mobility of the **DAE** core upon photoisomerization may induce alterations in the entire conformational space of the macrocycles. These changes are likely to result in efficient photocontrol of biological activity [39]. Thus, our aim in this work was to design, synthesize, and perform functional and structural characterization of several cyclic tubulysin analogues containing an appropriate **DAE**-derived side-chain/side-chain cross-linker (Figure 1c), similar to that used in one of our previous works [24]. We used the double Cu(I)-catalyzed azide-alkyne cycloaddition reaction (CuAAC), also known as a "click-reaction," between corresponding bis-azides and bis-alkynes for this purpose.

## 2 | Results

### 2.1 | Design of Photoswitchable Tubulysin Analogues

Introduction of a substantial **DAE** fragment into a tubulysin molecule, followed by macrocyclisation, would typically be expected to abolish biological activity. Therefore, before embarking on the synthesis, we performed careful design of the targeted tubulysin analogues. Based on published data on the structure of tubulysin ligands in their tubulin-bound state and structure–activity relationship (SAR) studies, we identified regions of the tubulysin core suitable for modification. These areas allowed the attachment of the **DAE**-containing linker without significantly affecting biological activity via the planned CuAAC cyclisation reaction. Below, we briefly discuss the data that influenced our decisions regarding the possible sites for the incorporation of azide-containing functional groups into the tubulysin core to prepare the precursors for the cyclisation.

### 2.2 | Structural Data Used in the Design

In 2010, Carlomagno and colleagues published a 3D structure of tubulysin A bound to tubulin [40]. The "biologically active" conformation was elucidated in this study by nuclear magnetic resonance (NMR) structural analysis using mostly nuclear Overhauser effect-derived data. The key contacts within the binding pocket and the biologically relevant conformation were further supported by an X-ray crystal structure of tubulysin M complexed with tubulin at 2.5 Å resolution, reported by Yang et al. [41]. The conformation of the tubulysin M N-terminus, where the interactions with the protein are strongest, matched that of tubulysin A as determined by Carlomagno and colleagues. Several further relevant X-ray structures were published after the synthesis of our target molecules had begun [42–44].

Critical insights from these structural studies are pivotal for designing photoswitchable tubulysin analogues. First, the tyrosylethyl, **Tuv** C5-acetyl, *O*-acyl *N*,*O*-acetal, γ-carboxy groups can be eliminated, and the piperidine ring can be slightly modified without affecting the primary tubulysin binding interactions with tubulin. Second, tubulysin molecules bind within a cleft between the $\alpha$ and $\beta$ subunits of two consecutively aligned tubulin dimers, with the **Ile** residue and the isopropyl group of the **Tuv** located in two hydrophobic pockets. Consequently, these residues should remain intact. Finally, for designing photoswitchable analogues, it is important to know that target protein interacts with both tubulysin A and tubulysin M via one face of these linear molecules. Therefore, the **DAE** fragment can be attached to the opposite face, where the **Tut/Tup** and **Mep** residues are located.

### 2.3 | Known SAR Data for Tubulysins Used in the Design Mep Residue Modifications

It has been demonstrated that replacing the **Mep** residue with other low-polar tertiary $\alpha$-amino acid residues, such as *N*-dimethylglycine or (*R*)-*N*-methylvaline, does not significantly affect biological activity [45–47]. NMR and X-ray structural data indicated that the **Mep** residue points outward from the binding pocket. We concluded, therefore, that the **Mep** residue can be simplified and modified with a side-chain bearing an azide group as shown in Figure 2a.

### 2.4 | Ile Residue Modifications

The relevance of the **Ile** residue in the tubulysin pharmacophore was extensively studied by Nicolaou and colleagues [47–49]. Their SAR analysis confirmed insights on the crucial role of this residue based on crystallographic results. It participates in two hydrogen bond interactions with the target protein, and its hydrophobic side-chain fits snugly into the $\alpha$2 tubulin subunit. Some $\beta$-branched moieties at the **Ile** position (isopropyl, tertiary

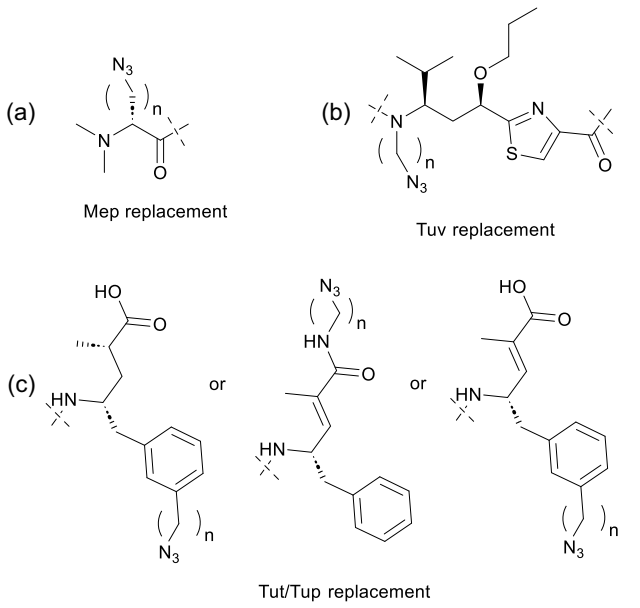


**FIGURE 2** | Possible replacements of the tubulysin residues to obtain the azide-containing precursors of the photoswitchable cyclic analogues. (a) Modifications of the **Mep** residue. (b) **Tuv** decorations by azide-containing group. (c) **Tut/Tup** alternatives.

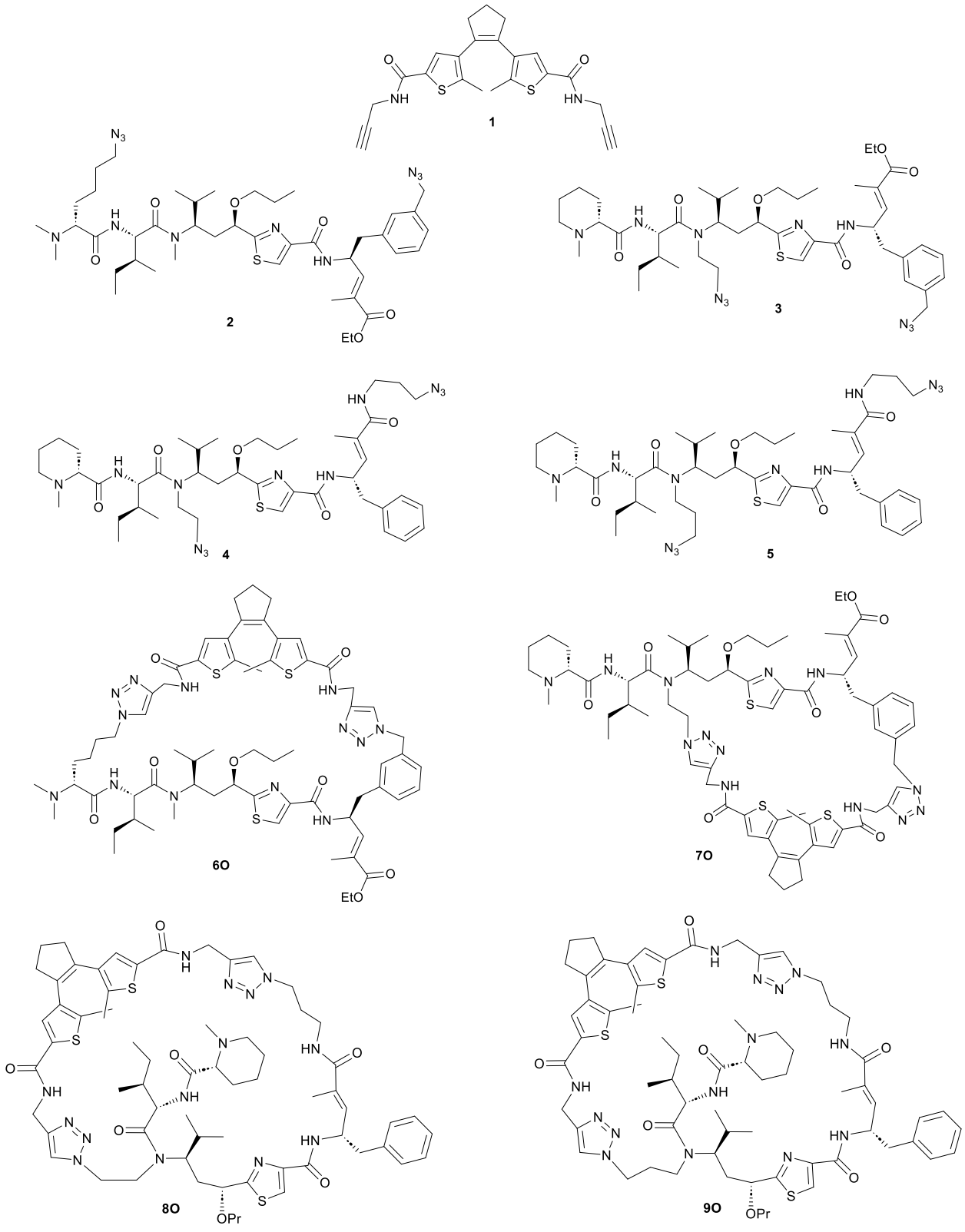


**FIGURE 3** | Designed linear precursors (**1–5**) and target cyclic molecules (**6O–9O**) selected for synthesis.

butyl, or 1,1-dimethylpropyl) are tolerated, and the corresponding tubulysin derivatives showed even improved antiproliferation potencies. On the other hand, longer n-butyl, 3-methylbutyl, or smaller methyl substituents instead of the isoleucine side-chain are not accepted, leading to significantly lower cytotoxicity of the corresponding analogues. Based on these results as well as on the structural data, we concluded that the **Ile** fragment cannot be modified to introduce a linker group in our design.

## 2.5 | Tuv Residue Modifications

The **Tuv** moiety is the most complex fragment in tubulysins. Its role in the tubulysin pharmacophore has been extensively studied. These studies revealed that the chemically labile and synthetically problematic *N*,*O*-acetal group is not required for biological activity and can be replaced by a methyl group with only a slight loss of activity [50]. In 2011, the Wessjohan group reported a robust approach towards the synthesis of tubulysin analogues called "TubUgis," where different **Tuv** N-substituents were introduced via an Ugi four-component reaction [51]. The tubulysin analogues with the *N*,*O*-acetal replaced by a glycine amide exhibited cytotoxic potency equal to that of tubulysin A. Kazmaier's and Müller's groups went further in attempting to simplify the structure of the **Tuv** residue and found that the acetoxy functionality is not critical for cytotoxicity at all and can be removed. A new simplified derivative named "pretubulysin" had only a modestly reduced activity compared to tubulysin D, still within the picomolar range [52]. The synthetic strategy for the *N*-substituted **Ile**-**Tuv** fragment was elaborated by the Kazmaier group, who introduced functionalized side-chains and determined that the *N*,*O*-acetal can be substituted with various nonpolar moieties without decreasing the biological potency [53]. Pillow et al. have shown that replacement of the acetate group in **Tuv** with a stable propyl ether (OPr) isostere retained potency, making this tubulysin derivative metabolically stable and efficient in vivo at the same time [54, 55]. Other modifications such as replacement of the thiazole group with a phenyl ring or other heterocyclic fragments (1,3-oxazoles, 1,2,3-triazole) led to a significant drop in potency [56]. Considering all of the above SAR data on the **Tuv** residue and published discoveries on synthetic and structural simplifications, we set out to synthesize a **Tuv**-derived building block possessing an azide-bearing substituent instead of the *N*,*O*-acetal group, as well as the OPr substituent instead of the acetoxy group (Figure 2b).

## 2.6 | Tut/Tup Residue Modifications

X-ray crystallographic studies have shown that the phenyl moiety of the C-terminal (**Tut/Tup**) fragment fits into a hydrophobic cavity, and that the carboxylate group forms a salt bridge within a tubulin unit. Notably, the **Tup**-binding domain is located at the periphery of the tubulin binding site and thus tolerates numerous modifications, provided that these changes do not disrupt binding interactions. This observation aligns with a SAR study, indicating that the deletion of the entire fragment led to only a 10–20-fold reduction in in vitro cytotoxicity [45]. Tubulysin analogues with

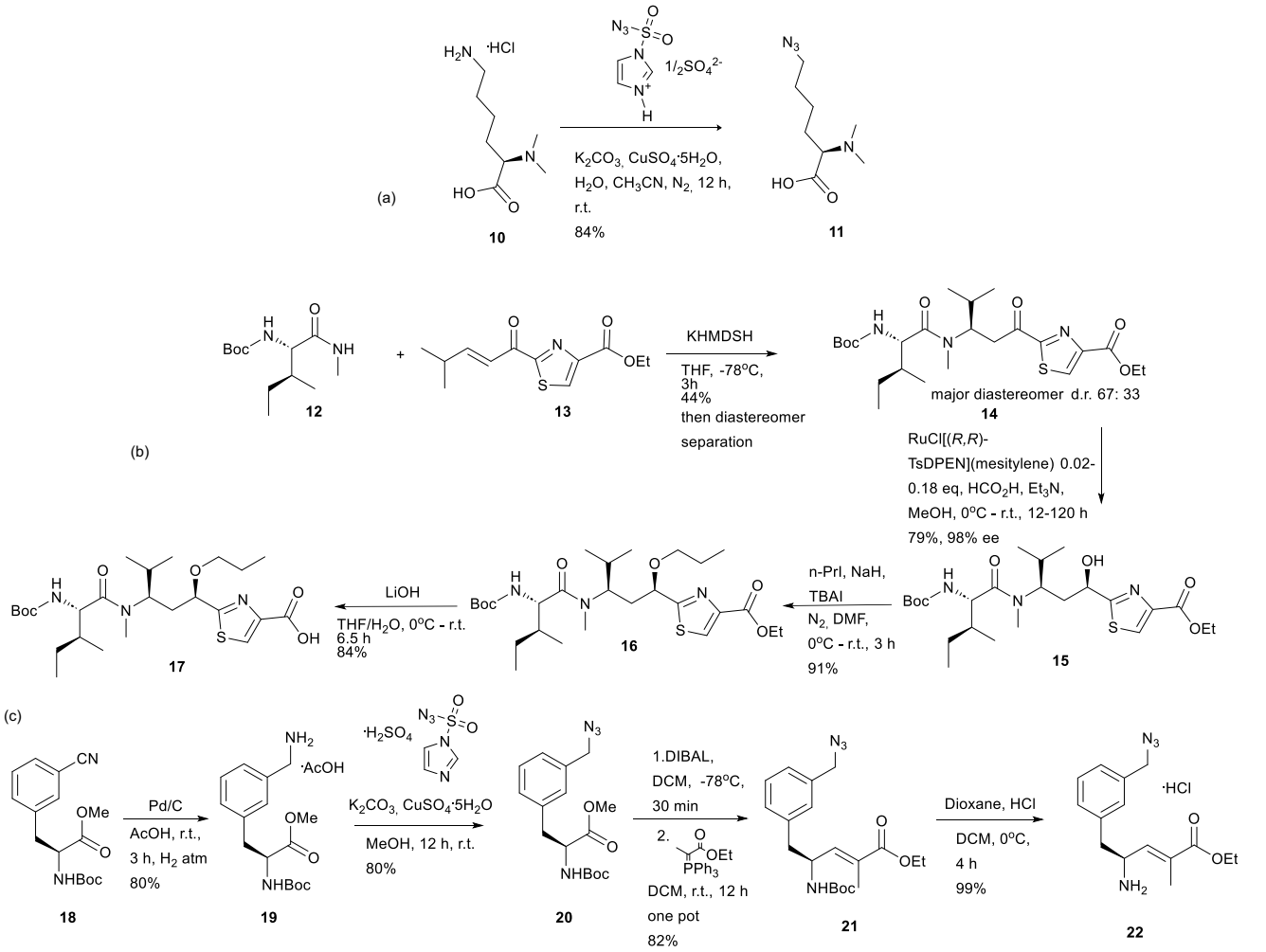


**SCHEME 1** | Synthesis of building blocks. (a) *N*-(2Me)-Lys-$N_3$. (b) Modified **Tuv**. (c) Modified **Tup**. Room temperature (r.t.) refers to ambient conditions.

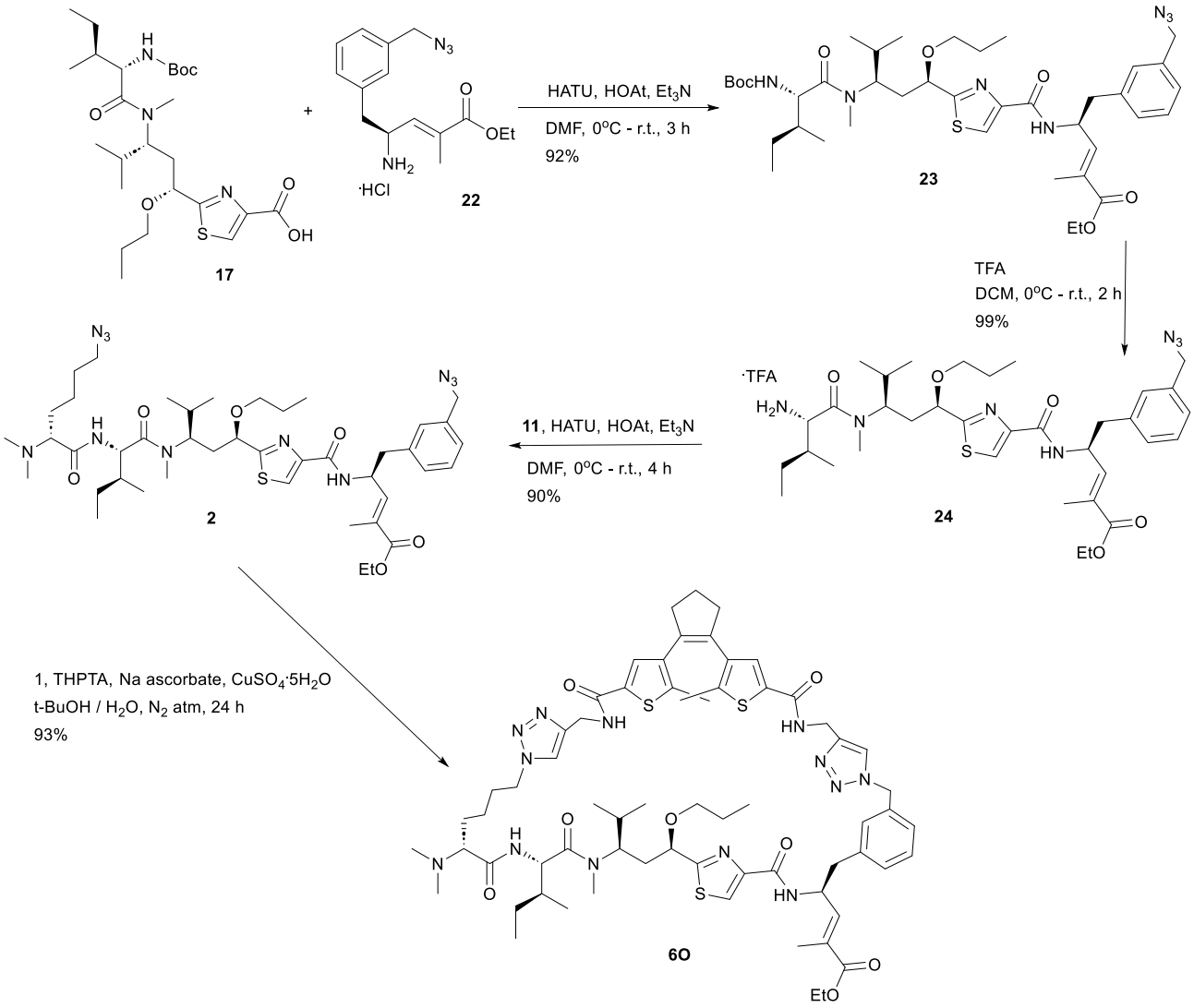


**SCHEME 2** | Synthesis of tubulysin analogue **6O**.

unsaturated versions of the **Tup** side-chain also demonstrated high biological activity [57]. Additionally, this modification was expected to streamline the synthesis of the modified **Tup**. Furthermore, replacing the C2 methyl group with nitrogen-containing substituents increased biological potency. These findings guided us on how to introduce azide-containing groups to attach the photoswitch without affecting critical binding interactions within this residue. Two modifications of the **Tup** residue were considered: meta-substitution of the phenyl ring by an azide-containing arm, and converting it to an unsaturated amide bearing the azide group, as illustrated in Figure 2c.

Taking the above considerations into account, we designed linear precursors **1–5** and cyclic **DAE**-containing tubulysin analogues **6O–9O** for synthesis (Figure 3). The cyclic tubulysin derivatives **6O** and **7O** feature the **DAE**-containing linker attached at the meta-position of the phenyl ring on one side, with different attachment points at the other side of the tubulysin core. Conversely, compounds **8O** and **9O** have the same attachment points for the **DAE**-derived linker to the tubulysin core but vary in the linker length. The modular structure of the target molecules and their structural similarities allowed us to use common synthetic precursors.

## 2.7 | Synthesis of the Target Compounds

### *2.7.1* | *Synthesis of 6O*

Synthesis of compound **6O** began with the preparation of three essential building blocks: *N*-(2Me)-Lys-$N_3$, modified tubuvaline (**Tuv**), and modified tubuphenylalanine (**Tup**), which are also utilized in the synthesis of other analogues.

The azidolysine derivative *N*-(2Me)-Lys-$N_3$ (**11**) was synthesized from compound **10** through an azido transfer reaction, as shown in Scheme 1a.

Scheme 1b illustrates the synthesis of the **Tuv** fragment. The Aza-Michael reaction of the isoleucine derivative **12** with $\alpha,\beta$-unsaturated thiazolyl ketone **13** [58] yielded a diastereomeric mixture of products (d.r. 67:33). These products were then separated, and the desired diastereomer **14** was obtained in moderate yield. The carbonyl group in compound **14** was subsequently reduced under conditions of enantioselective Noyori reduction to yield compound **15**. The modified **Tuv** building block **17**

was prepared by alkylating compound **15** with n-propyl iodide, followed by hydrolysing the resulting product **16**.

The modified **Tup** was synthesized from compound **18** through a series of steps: reduction of the nitrile group, azido transfer reaction, a one-pot methyl ester reduction with diisobutylaluminium hydride, Wittig reaction, and *tert*-butyloxycarbonyl (Boc) N-deprotection, as outlined in Scheme 1c.

With the necessary building blocks prepared, we proceeded with the synthesis of the linear tubulysin analogue **2**. The reaction sequence, illustrated in Scheme 2, included coupling compounds **17** and **22**, followed by Boc deprotection and subsequent coupling with azidolysine **11**. The final step in synthesizing the target cyclic tubulysin analogue **6O** involved a "double-click" reaction of **2** with the bis-alkyne **1**, successfully generating the **DAE**-containing tubulysin **6O**.

### 2.7.2 | *Synthesis of 7O*

To synthesize compound **7O**, we used a modified **Tuv** precursor **36**, the synthesis of which is detailed in Scheme 3. Similarly, homologue **37** was synthesized for later use in the synthesis of **9O**. The synthetic approach followed the strategy outlined previously for obtaining modified tubuvaline **17**. The subsequent steps involved sequential coupling, *N*-Boc deprotection, and a "double-click" reaction, as illustrated in Scheme 3. The successful execution of these steps ensured the controlled assembly of the tubulysin derivative **7O**, possessing the desired structural characteristics.

### 2.7.3 | *Synthesis of Compounds 8O and 9O*

Tubulysin analogues **8O** and **9O** were obtained using a similar multistep approach. Key steps involved the coupling reactions of compounds **36** or **37** with **41** (obtained according to literature) [52], *N*-Boc-deprotection, successive coupling reactions, ethyl

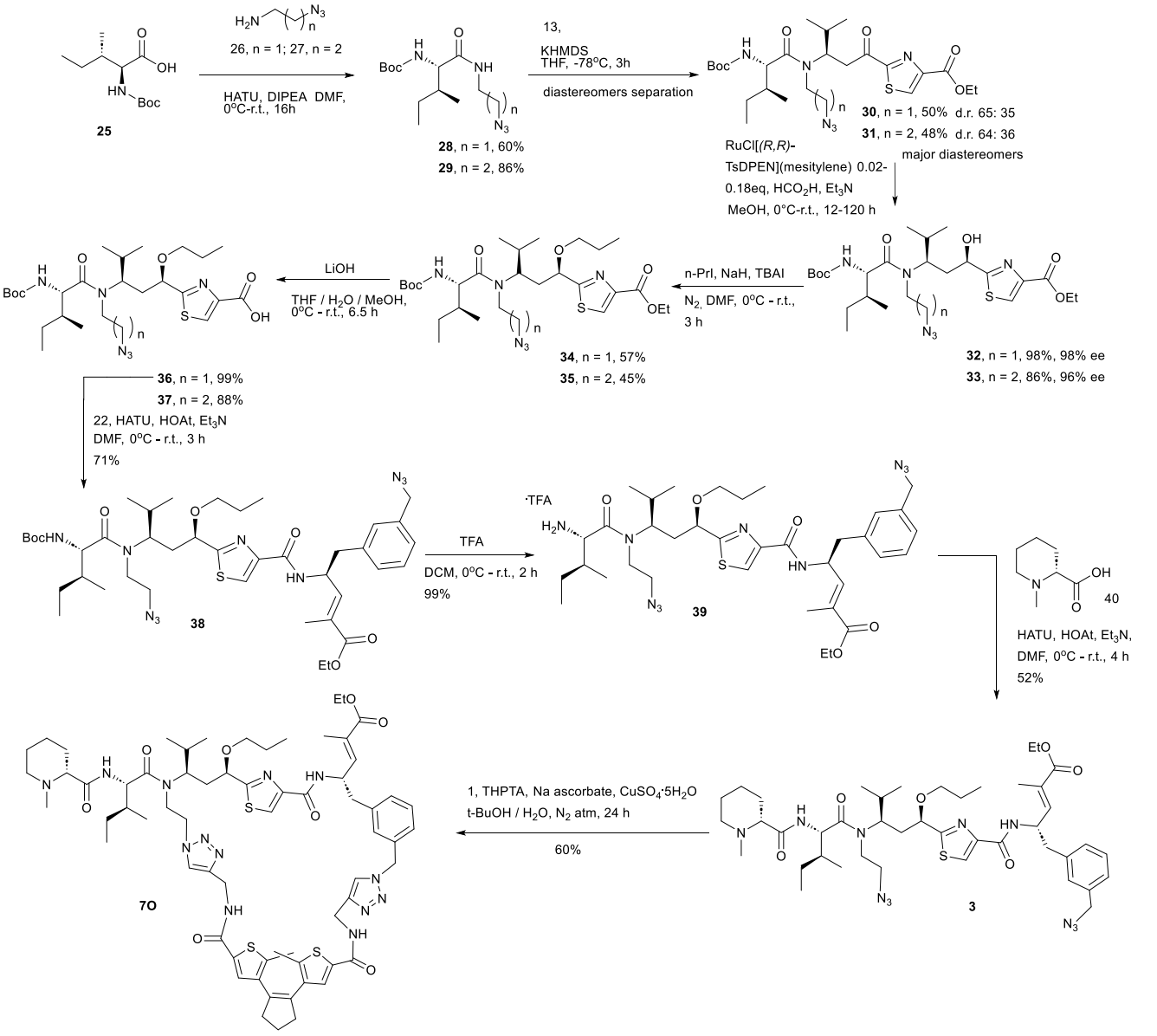


**SCHEME 3** | Synthesis of tubulysin analogue **7O**.

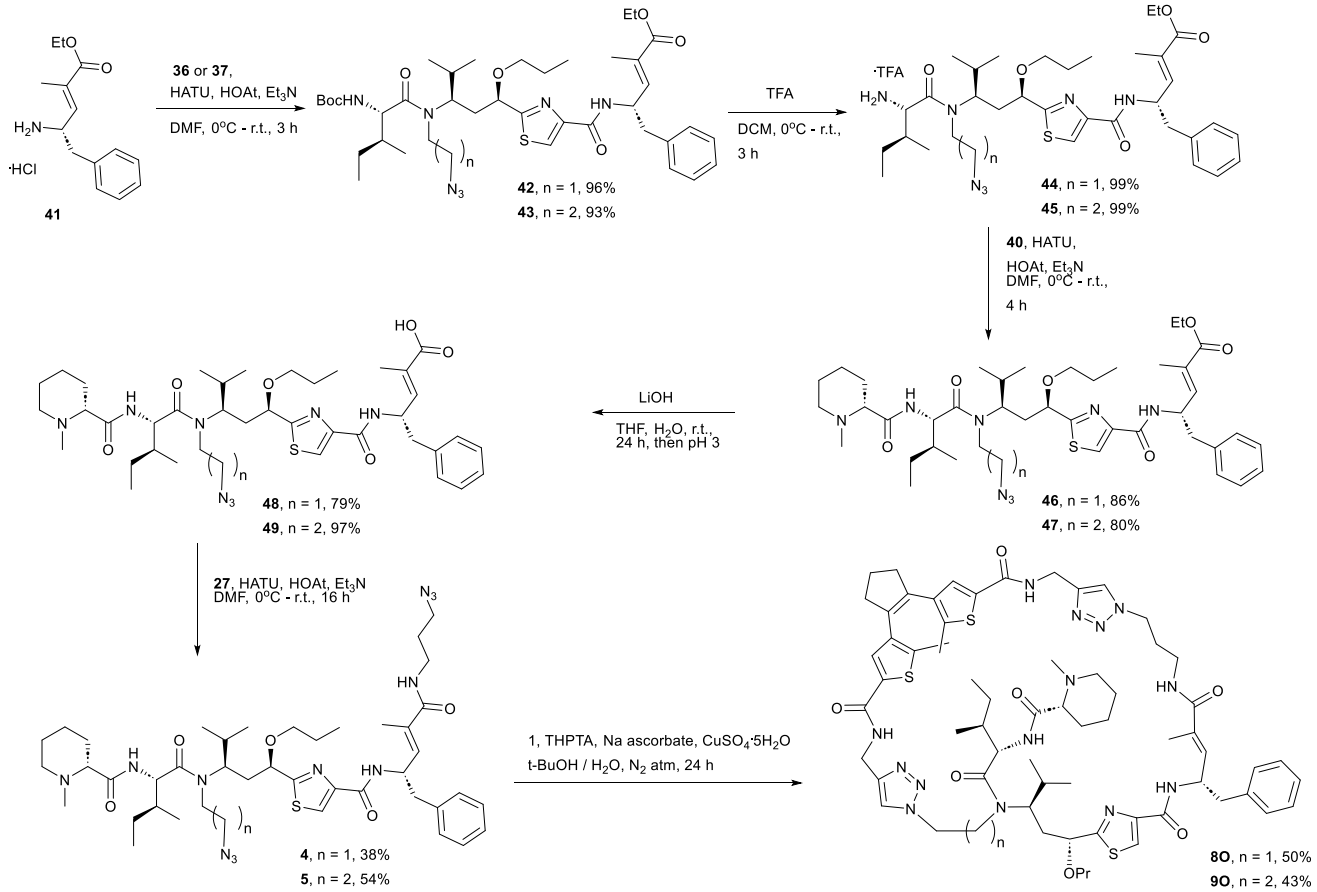


**SCHEME 4** | Synthesis of tubulysin analogues **8O** and **9O**.

ester hydrolysis, and coupling with azidoamine **27**, followed by a final "double-click" reaction (Scheme 4).

## 2.8 | Photoisomerization of the DAE-Containing Tubulysin Analogues

Having successfully synthesized the cyclic **DAE**-containing tubulysin analogues in their open form, we proceeded with their ultraviolet light (UV)-induced photoisomerization into the closed form. The progress of this reaction was monitored using high-performance liquid chromatography. Unfortunately, compounds **6O–8O** showed no efficient photoconversion under various conditions (varying solvents, light dose, concentrations, and denaturating agents). This observation suggests that the cyclic structure of these compounds may adopt conformations that are unfavourable for the open-to-closed cyclysation reaction. Similar structural and dynamic constraints that hinder open-to-closed photoisomerization have been reported for macrocyclic peptides containing relatively small **DAE**-based loops [24, 59]. In general, smaller macrocycles are more likely to restrict the conformational changes required for the open-to-closed photoisomerization. Our previous study showed, for example, that **DAE**-containing cyclic peptidomimetics with 26 atoms in the macrocycle did not photoisomerize, whereas analogous 58-membered macrocycles underwent efficient photoconversion [59]. The compounds examined here, **6O–9O**, contain 41–46 atoms in their macrocycles, placing them in an intermediate size range. Therefore, even relatively small structural changes may strongly affect their photochemical behaviour.

Fortunately, compound **9O**, with an elongated **DAE**-containing linker, could be converted smoothly to its closed photoform upon UV irradiation (Scheme 5). The photostationary state was established in ≈70 min under the conditions used, resulting in an open:closed ratio of ≈75:25. The pure closed photoisomer **9C** was obtained by chromatographic purification in the dark. Analysis of the X-ray data (*vide infra*) reveals that the isolated major diastereomer possesses the (*R*,*R*)-configuration of the stereogenic carbon atoms in the diarylethene fragment. The reverse photoconversion to the **9O** isomer was nearly complete upon red-light-emitting diode irradiation of the compound in saturated aqueous urea solution for ≈2 h ($\lambda_{max} = 640$ nm, light power density ~50 mW/cm$^2$).

## 2.9 | Biological Activity of the Photoswitchable Tubulysins

The photoisomers of the cyclic tubulysin analogue that demonstrated good photoswitching ability (compounds **9O** and **9C**) were tested in a fluorescence-based tubulin polymerization assay to evaluate their ability to interfere with microtubule formation. The linear precursor **5** and tubulysin M were also tested for comparison. The resulting $IC_{50}$ and $EC_{50}$ values are summarized in Table 1.

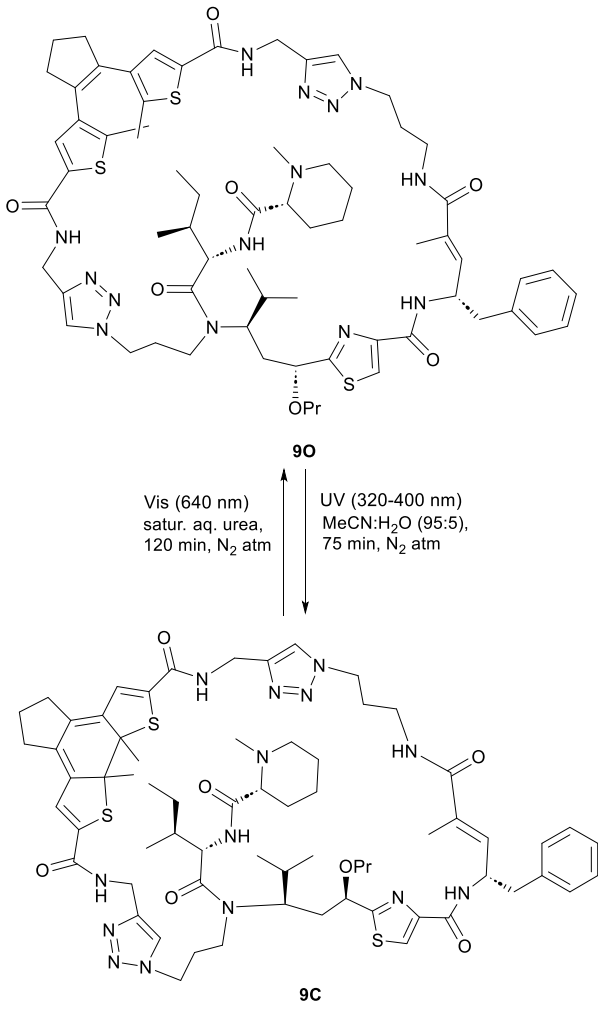


**SCHEME 5** | Photoswitching of tubulysin analogue **9O**.

We were pleased to find that one photoisomer, **9C**, exhibited activity comparable to tubulysin M in the in vitro tubulin polymerization assay, while the other photoisomer, **9O**, was significantly less active in interfering with tubulin polymerization. The linear precursor **5** also showed activity similar to tubulysin M. These results validate our design, demonstrating that the attachment points in the tubulysin molecule for the photoisomerizable linker preserved the tubulysin pharmacophore and allowed for efficient photoregulation of tubulin polymerization.

Notably, the more active closed form, **9C**, is generated by UV light, whereas the less active open form, **9O**, is formed from **9C** upon irradiation with red light. This behaviour is suitable for photopharmacology applications where drug deactivation by light is desirable after the drug has exerted its function, as discussed in the literature [3, 4, 60]. The post-treatment drug deactivation in patients under daylight could potentially alleviate problems of phototoxicity, expected for photopharmacological treatment and common for similar treatment modality, photodynamic therapy [61].

Additionally, we aimed to investigate whether the differential activities of tubulysin analogues **9O** and **9C** in tubulin polymerization inhibition were also mirrored in cell viability assays. The cytotoxicity of these **DAE**-containing derivatives was assessed using HEK-293T (Human Embryonic Kidney) and MCF-7 (Michigan Cancer Foundation-7, human breast adenocarcinoma) cell lines, with tubulysin M and compound **5** as controls. The results, illustrated in Table 1, indicate that the **DAE**-containing derivatives exhibit cytotoxic activity, albeit lower compared to their linear analogues. Nevertheless, the cell viability assay results align with those from the tubulin polymerization assay. Specifically, the greater potency of **9C** (the closed photoform) relative to **9O** (the open photoform) was confirmed. These data demonstrate that the cytotoxic activity of the photoisomerizable analogue can be regulated by light, with approximately a six-fold difference in $IC_{50}$ values between its two photoisomeric forms. The reduced activity of both **9O** and **9C** compared to the parent tubulysin in cell assays, despite similar tubulin binding activities, may be attributed to the lower cell-penetrating ability of the new analogues.

## 2.10 | X-Ray Crystallography Studies of Complexes of Photoswitchable Tubulysin with Tubulin

To understand molecular features underlying the differences in biological activities of the open and closed isomers **9O** and **9C**, we performed X-ray crystallography of $T_2$R-TTL complexes [62, 63] bound to both compounds, as well as to the linear precursor, compound **5**. The $T_2$R-TTL protein complex is composed of two $\alpha\beta$-tubulin heterodimers ($T_2$), the stathmin-like protein RB3 (R), and tubulin tyrosine ligase (TTL). The complex contains one accessible vinca site at the interdimer interface of two consecutively aligned tubulin dimers, and one exposed $\beta$-tubulin surface on the second tubulin dimer. The crystal structures of the three $T_2$R-TTL-compound complexes were determined to 2.5 Å (**5**, **9C**) and 3.3 Å (**9O**) resolutions, respectively (Supplementary Table S1). To the best of our knowledge, crystal structures of the complexes with **9O** and **9C** represent the first X-ray crystallography study comparing two complexes of a

**TABLE 1** | Tubulin polymerization and cell viability assays.

| | Tubulin polymerization | | Cell viability | |
|---|---|---|---|---|
| **Compound** | **$IC_{50}$, μM** | **$EC_{50}$, μM** | **$IC_{50}$, μM HEK-293T** | **$IC_{50}$, μM MCF-7** |
| **Tubulysin M** | 3.2 | ~2 | 0.0003 | 0.0004 |
| **5** | 3.2 | ~4 | 0.081 | 0.066 |
| **9O** | 15.4 | ~22 | 3.379 | 6.009 |
| **9C** | 3.1 | ~2 | 0.593 | 0.957 |

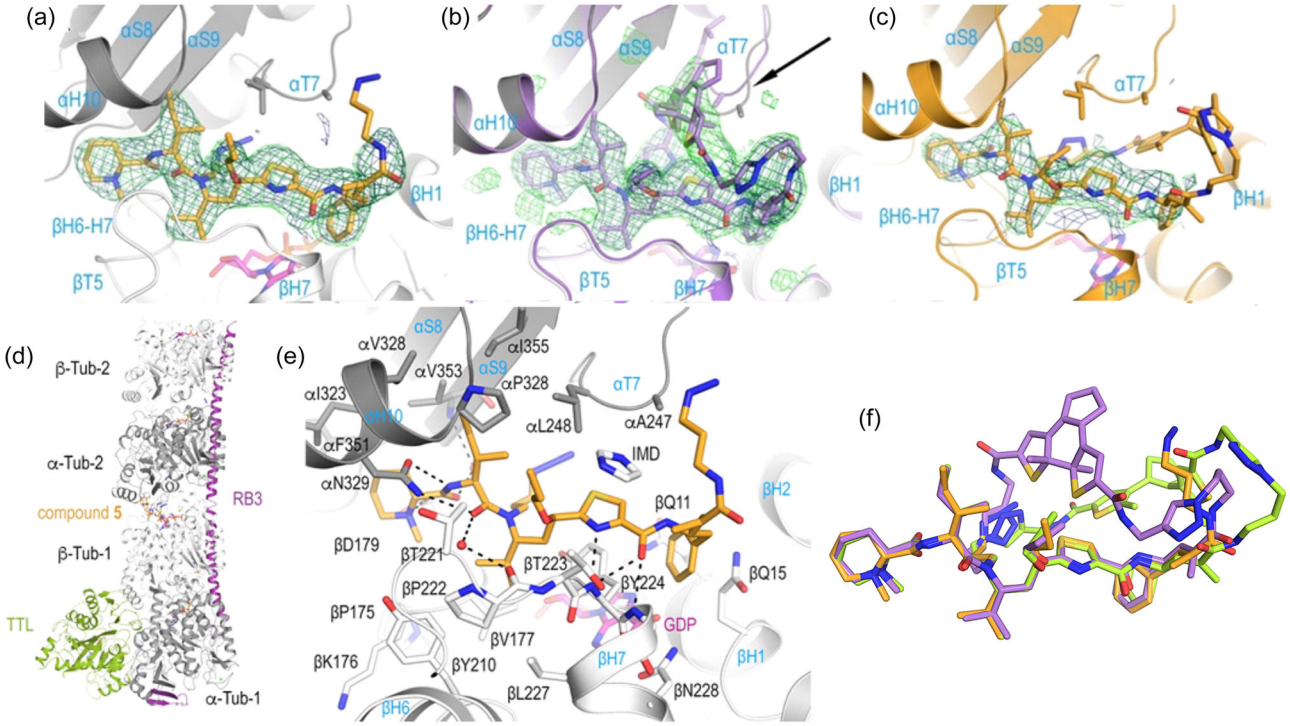


**FIGURE 4** | X-ray crystallography of $T_2$R-TTL–compound complexes. (a–c) Electron density omit maps of the vinca-sites of the tubulin-**5** (a), tubulin-**9C** (b), and tubulin-**9O** (c) complex structures. [SigmaA-weighted 2mFo-DFc (dark blue mesh) and mFo-DFc (light green mesh) omit maps are contoured at +1.0 $\sigma$ and +3.0 $\sigma$, respectively. Models of the individual ligands are superimposed to the maps and coloured.] (d) Overview of binding pose of **5** within the vinca site. [Ribbon representation of the $T_2$R–TTL complex—the α- and β-tubulin chains are coloured in dark and light grey, respectively, TTL is coloured in olive green, and RB3 in purple. The bound compound **5** (cheddar orange) is displayed in stick representation.] (e) Close-up view of the distinct binding pose of **5** in the vinca site, using the same colour code as in (d). Ligands and interacting residues are in stick representation and are labelled and coloured according to their chain assignment; oxygen atoms and nitrogen atoms are coloured red and blue, respectively. Secondary structure elements are indicated in blue font. Superimposed structure models for **5** (cheddar orange), **9O** (lime green), and **9C** (lavender purple) in their bound states (f).

**DAE**-containing photoswitchable molecule bound to a protein, contrasting both its open and closed photoforms.

For all three compounds, **5**, **9C**, and **9O**, we detected binding to the vinca site of tubulin at the interdimer interface, which comprises residues from strand $\alpha$S8, helix $\alpha$H10, and the loop $\alpha$T7 of $\alpha$-tubulin, as well as from loops $\beta$T5 and $\beta$H6-H7, and helices $\beta$H1 and $\beta$H7 of $\beta$-tubulin (Figure 4). This is consistent with other structural studies with peptide-based vinca-site binders [41, 64]. The binding pose superimposes well (rmsd 0.224 Å over 398 C$\alpha$-atoms of $\beta$-tubulin) with the one described by Wang et al. for tubulysin M (PDB ID 4ZOL) [41]. Clear electron density defining the core tubulysin moiety was detected for all three compounds at the interdimer interface (Figure 4a–c), whereas no difference density was observed at the exposed site on $\beta$-tubulin.

In the difference electron density omit map of the $T_2$R-TTL-**9C** structure, additional density was observed near the $\alpha$T7-loop, likely corresponding to the diarylethene moiety. This suggests that the closed compound perturbs the $\alpha$T7-loop (Figure 4b, the perturbed region is indicated by an arrow). However, due to substantial level of perturbation in this region, the bound model of **9C** could not be refined with higher confidence. For $T_2$R-TTL-**9O**, the difference electron density omit map was poorly defined, showing only the core moiety of the parent compound, with no detectable density for the photoswitch moiety. Thus, the open compound is not affecting the $\alpha$T7-loop. Figure 4f shows an overlay of the structure models for compounds **5**, **9O**, and **9C** in their bound states, revealing clear conformational differences among the poses of the photoswitchable moieties of the ligands. In conclusion, the differences observed between the electron density maps of **9C** and **9O** correlate with their observed biological activities.

## 3 | Discussion

The functional tests and X-ray data described in the manuscript provide several important lessons. In vitro assays on the molecular target showed that one DAE analogue retained activity comparable to tubulysin M, which was an encouraging result. However, the cell-based assays, which are more relevant to potential in vivo applications, were less satisfactory. Both **9O** and **9C** turned out to be three orders of magnitude less active than tubulysin M. These results highlight the following key points: (i) even for compounds whose biological activity is highly sensitive to structural modification, carefully designed photoswitchable **DAE** analogues can retain high affinity for the biological target. The design should strictly follow the principles derived from our experimental results. Namely, the modification should provide cyclic molecules with a ring size of 44 atoms and

more, to achieve photoswitching. They also must avoid those regions of the template molecule which are essential for biological activity; (ii) successful incorporation of a **DAE** photoswitch, strong affinity for a molecular target and efficient photoswitching do not necessarily ensure success in cellular or in vivo applications. This is a common challenge in drug design, and further optimization strategies depend on the underlying cause of the reduced performance. In our case, we suspect that the tested **DAE**-modified compounds have limited cell permeability. Noticeably, compound **5** (a linear precursor of **9O/9C** without the photoswitch) is only two orders of magnitude less active than tubulysin M, suggesting that the photoswitch-containing linker contributes considerably to the activity loss. Further studies are needed to verify this hypothesis. If confirmed, possible optimization could include, for example, attachment of a cell-penetrating peptide fragment; (iii) X-ray data are particularly useful for interpreting differences in biological activity between photoisomers when the target protein can be crystallized in complex with both forms of the photoswitchable ligand. In our case, the structural data revealed that a crucial interaction with a protein loop involves the **DAE** fragment. This interaction may explain the observed "reverse" bioactivity switch, in which the closed form is more active than the open form. Such behaviour is uncommon: for most **DAE**-derived peptidomimetics, the open forms have been reported to be more active than the corresponding closed forms. In our case, the closed form of the photoswitch interacts with the $\alpha$T7-loop that can explain higher activity of this photoisomer. Consequently, the X-ray data suggest that shifting the **DAE** fragment toward one end of the cyclisation linker could help achieve a "normal" bioactivity switch and may improve the overall results.

## 4 | Conclusions

We have successfully designed and synthesized novel cyclic tubulysin analogues by incorporating a **DAE** photoswitch into the modified tubulysin core. We identified the optimal positions for this photoswitch, which retains the tubulin-binding and cytotoxic activities of these compounds while at the same time enabling efficient photoregulation of their activity. Our synthetic efforts led to a significant six-fold difference in potency between the two photoforms of one compound (**9O**, **9C**). For the first time, through a comparison of X-ray crystallography data for both isomeric photoforms of a **DAE**-modified bioactive compound bound to the protein target, we have elucidated the variations in their biological activities. These findings may serve as a starting point for developing safer photopharmacology therapies against cancer and further advance the development of peptide-based photocontrollable tools for chemical biology and medicinal chemistry applications.


### Acknowledgments

The authors acknowledge EU funding by the H2020-MSCA RISE program ALISE (#101007256). We also acknowledge Diamond Light Source for time on Beamline I03 under Proposal mx-34035. This work was partially supported by the Swiss National Science Foundation (grant 310030_192566; to M.O.S.).

### Funding

This study was supported by the H2020 Marie Skłodowska-Curie Actions (101007256), and Schweizerischer Nationalfonds zur Förderung der Wissenschaftlichen Forschung (310030_192566).


### Conflicts of Interest

The authors declare no conflicts of interest.

### Data Availability Statement

The coordinates and structure factors of the $T_2$R-TTL-**5** complex were deposited at the Protein Data Bank (RCSB PDB, www.rcsb.org) under accession number PDB: 9R2X. Further data that support the findings of this study are available from the corresponding authors upon reasonable request.

### References


1. J. Broichhagen, J. A. Frank, and D. Trauner, "A Roadmap to Success in Photopharmacology," *Accounts of Chemical Research* 48 (2015): 1947.

2. W. Szymański, J. M. Beierle, H. A. V. Kistemaker, W. A. Velema, and B. L. Feringa, "Reversible Photocontrol of Biological Systems by the Incorporation of Molecular Photoswitches," *Chemical Reviews* 113 (2013): 6114.

3. W. Velema, W. Szymanski, and B. L. Feringa, "Photopharmacology: Beyond Proof of Principle," *Journal of the American Chemical Society* 136 (2014): 2178.

4. K. Hüll, J. Morstein, and D. Trauner, "In Vivo Photopharmacology," *Chemical Reviews* 118 (2018): 10710.

5. O. Babii, S. Afonin, T. Schober, et al., "Peptide Drugs for Photopharmacology: How Much of a Safety Advantage Can Be Gained by Photocontrol?," *Future Drug Discovery* 2 (2020): FDD28.

6. M. J. Fuchter, "On the Promise of Photopharmacology Using Photoswitches: A Medicinal Chemist's Perspective," *Journal of Medicinal Chemistry* 63 (2020): 11436.

7. F. Sasse, H. Steinmetz, J. Heil, G. Höfle, and H. Reichenbach, "Tubulysins, New Cytostatic Peptides From, *Myxobacteria*, Acting on Microtubuli. Production, Isolation, Physico-Chemical and Biological Properties," *The Journal of Antibiotics* 53 (2000): 879.

8. Y. Chai, D. Pistorius, A. Ullrich, K. J. Weissman, U. Kazmaier, and R. Müller, "Discovery of 23 Natural Tubulysins From, *Angiococcus disciformis*, An d48 and, *Cystobacter* SBCb004," *Chemistry & Biology* 17 (2010): 296.

9. B. C. Murray, M. T. Peterson, and R. A. Fecik, "Chemistry and Biology of Tubulysins: Antimitotic Tetrapeptides With Activity Against Drug Resistant Cancers," *Natural Product Reports* 32 (2015): 654.

10. M. W. Khalil, F. Sasse, H. Lünsdorf, Y. A. Elnakady, and H. Reichenbach, "Mechanism of Action of Tubulysin, an Antimitotic Peptide From *Myxobacteria*," *ChemBioChem* 7 (2006): 678.

11. P. Khongorzul, C. J. Ling, F. U. Khan, A. U. Ihsan, and J. Zhang, "Antibody-Drug Conjugates: A Comprehensive Review," *Molecular Cancer Research* 18 (2020): 3–19.

12. X. Wang, C. Guo, J. Shao, et al., "Small Molecule-Drug Conjugates: An Emerging Drug Design Strategy for Targeted Therapeutics," *Journal of Medicinal Chemistry* 68 (2025): 24759–24784.

13. J. Hoffmann and U. Kazmaier, "A Straightforward Approach Towards Cyclic Photoactivatable Tubulysin Derivatives," *Angewandte Chemie International Edition* 53 (2014): 11356.

14. O. Babii, S. Afonin, M. Berditsch, et al., "Controlling Biological Activity With Light: Diarylethene-Containing Cyclic Peptidomimetics," *Angewandte Chemie International Edition* 53 (2014): 3392.

15. O. Babii, S. Afonin, L. V. Garmanchuk, et al., "Direct Photocontrol of Peptidomimetics: An Alternative to Oxygen-Dependent Photodynamic Cancer Therapy," *Angewandte Chemie International Edition* 55 (2016): 5493.

16. O. Babii, S. Afonin, A. Y. Ishchenko, et al., "Structure–Activity Relationships of Photoswitchable Diarylethene-Based $\beta$-Hairpin Peptides as Membranolytic Antimicrobial and Anticancer Agents," *Journal of Medicinal Chemistry* 61 (2018): 10793.

17. Z. Li, Y. Wang, M. Li, et al., "Synthesis and Properties of Dithienylethene-Functionalized Switchable Antibacterial Agents," *Organic & Biomolecular Chemistry* 16 (2018): 6988.

18. D. Vomasta, C. Högner, N. Branda, and B. König, "Regulation of Human Carbonic Anhydrase I (hCAI) Activity by Using a Photochromic Inhibitor," *Angewandte Chemie International Edition* 47 (2008): 7644.

19. C. Falenczyk, M. Schiedel, B. Karaman, et al., "Chromo-Pharmacophores: Photochromic Diarylmaleimide Inhibitors for Sirtuins," *Chemical Science* 5 (2014): 4794.

20. A. C. Kneuttinger, M. Winter, N. A. Simeth, et al., "Artificial Light Regulation of an Allosteric Bienzyme Complex by a Photosensitive Ligand," *ChemBioChem* 19 (2018): 1750.

21. O. Babii, S. Afonin, C. Diel, et al., "Diarylethene-Based Photoswitchable Inhibitors of Serine Proteases," *Angewandte Chemie International Edition* 60 (2021): 21789.

22. B. Reisinger, N. Kuzmanovic, P. Löffler, et al., "Exploiting Protein Symmetry to Design Light-Controllable Enzyme Inhibitors," *Angewandte Chemie International Edition* 53 (2014): 595.

23. D. Wilson, J. W. Li, and N. R. Branda, "Visible-Light-Triggered Activation of a Protein Kinase Inhibitor," *ChemMedChem* 12 (2017): 284.

24. A. V. Strizhak, O. Babii, S. Afonin, et al., "Diarylethene Moiety as an Enthalpy–Entropy Switch: Photoisomerizable Stapled Peptides for Modulating p53/MDM2 Interaction," *Organic & Biomolecular Chemistry* 18 (2020): 5359.

25. T. Schober, I. Wehl, S. Afonin, et al., "Controlling the Uptake of Diarylethene-Based Cell-Penetrating Peptides Into Cells Using Light," *ChemPhotoChem* 3 (2019): 384.

26. A. Müller-Deku, J. C. M. Meiring, K. Loy, et al., "Photoswitchable Paclitaxel-Based Microtubule Stabilisers Allow Optical Control Over the Microtubule Cytoskeleton," *Nature Communications* 11 (2020): 4640.

27. L. Gao, J. C. Meiring, C. Heise, et al., "Photoswitchable Epothilone-Based Microtubule Stabilisers Allow GFP-Imaging-Compatible, Optical Control Over the Microtubule Cytoskeleton," *Angewandte Chemie International Edition* 61 (2022): e202114614.

28. M. Borowiak, W. Nahaboo, M. Reynders, et al., "Photoswitchable Inhibitors of Microtubule Dynamics Optically Control Mitosis and *Cell* Death," *Cell* 162 (2015): 403.

29. A. J. Engdahl, E. A. Torres, S. E. Lock, et al., "Synthesis, Characterization, and Bioactivity of the Photoisomerizable Tubulin Polymerization Inhibitor Azo-Combretastatin A4," *Organic Letters* 17 (2015): 4546.

30. J. E. Sheldon, M. M. Dcona, C. E. Lyons, J. C. Hackett, and M. C. Hartman, "Photoswitchable Anticancer Activity, *via*, Trans–Cis Isomerization of a Combretastatin a-4 Analog," *Organic & Biomolecular Chemistry* 14 (2016): 40.

31. S. K. Rastogi, Z. Zhao, M. B. Gildner, et al., "Synthesis, Optical Properties and, In Vitro, Cell Viability of Novel Spiropyrans and Their Photostationary States," *Tetrahedron* 80 (2021): 131854.

32. A. Sailer, F. Ermer, Y. Kraus, et al., "Hemithioindigos for Cellular Photopharmacology: Desymmetrised Molecular Switch Scaffolds Enabling Design Control Over the Isomer-Dependency of Potent Antimitotic Bioactivity," *ChemBioChem* 20 (2019): 1305.

33. A. Sailer, J. C. M. Meiring, C. Heise, et al., "Pyrrole Hemithioindigo Antimitotics With Near-Quantitative Bidirectional Photoswitching that Photocontrol Cellular Microtubule Dynamics With Single-Cell Precision," *Angewandte Chemie International Edition* 60 (2021): 23695.

34. L. Gao, J. C. Meiring, A. Varady, et al., "In Vivo Photocontrol of Microtubule Dynamics and Integrity, Migration and Mitosis, by the Potent GFP-Imaging-Compatible Photoswitchable Reagents SBTubA4P and SBTub2M," *Journal of the American Chemical Society* 144 (2022): 5614.

35. M. Borowiak, F. Küllmer, F. Gegenfurtner, et al., "Optical Manipulation of F-Actin With Photoswitchable Small Molecules," *Journal of the American Chemical Society* 142 (2020): 9240.

36. S. Dani, K. Schütz, E. Dikici, A. Bernhardt, and A. Lode,, "The Effect of Continuous Long-Term Illumination With Visible Light in Different Spectral Ranges on Mammalian Cells," *Scientific Reports* 14 (2024): 9444.

37. K. Fujimoto, M. Kajino, I. Sakaguchi, and M. Inouye, "Photoswitchable, DNA-Binding Helical Peptides Assembled With Two Independently Designed Sequences for Photoregulation and DNA Recognition," *Chemistry A European Journal* 18 (2012): 9834.

38. K. Fujimoto, T. Maruyama, Y. Okada, T. Itou, and M. Inouye, "Development of a New Class of Photochromic Peptides by Using Diarylethene-Based Non-Natural Amino Acids," *Tetrahedron* 69 (2013): 6170.

39. I. V. Komarov, S. Afonin, O. Babii, T. Schober, and A. S. Ulrich, "Efficiently Photocontrollable or Not? Biological Activity of Photoisomerizable Diarylethenes," *Chemistry – A European Journal* 24 (2018): 11245.

40. K. Kubicek, S. K. Grimm, J. Orts, F. Sasse, and T. Carlomagno, "The Tubulin-Bound Structure of the Antimitotic Drug Tubulysin," *Angewandte Chemie International Edition* 49 (2010): 4809.

41. Y. Wang, F. W. Benz, Y. Wu, et al., "Structural Insights Into the Pharmacophore of Vinca Domain Inhibitors of Microtubules," *Molecular Pharmacology* 89 (2016): 233.

42. C. A. Leverett, S. C. K. Sukuru, B. C. Vetelino, et al., "Stabilizing a Tubulysin Antibody–Drug Conjugate to Enable Activity Against Multidrug-Resistant Tumors," *ACS Medicinal Chemistry Letters* 7 (2016): 999.

43. W. Li, L. Tan, Z. Zhang, et al., "The X-Ray Structure of Tubulysin Analogue TGL in Complex With Tubulin and Three Possible Routes for the Development of Next-Generation Tubulysin Analogues," *Biochemical and Biophysical Research Communications* 565 (2021): 29.

44. W. Chengyong, X. Jinghong, W. Yanyan, et al., "The High-Resolution X-Ray Structure of Vinca-Domain Inhibitors of Microtubules Provides a Rational Approach for Drug Design," *FEBS Letters* 595 (2021): 195.

45. A. W. Patterson, H. M. Peltier, F. Sasse, and J. A. Ellman, "Design, Synthesis, and Biological Properties of Highly Potent Tubulysin D Analogues," *Chemistry A European Journal* 13 (2007): 9534.

46. C. Raffaele, W. Zhiyong, H. Junyan, et al., "Total Synthesis and Biological Evaluation of Tubulysin Analogues," *Journal of Organic Chemistry* 81 (2016): 10302.

47. K. C. Nicolaou, S. Pan, K. K. Pulukuri, et al., "Design, Synthesis, and Biological Evaluation of Tubulysin Analogues, Linker-Drugs, and Antibody–Drug Conjugates, Insights Into Structure–Activity Relationships, and Tubulysin–Tubulin Binding Derived From X-Ray Crystallographic Analysis," *Journal of Organic Chemistry* 86 (2021): 3377.

48. K. C. Nicolaou, J. Yin, D. Mandal, et al., "Total Synthesis and Biological Evaluation of Natural and Designed Tubulysins," *Journal of the American Chemical Society* 138 (2016): 1698.

49. K. C. Nicolaou, R. D. Erande, J. Yin, et al., "Improved Total Synthesis of Tubulysins and Design, Synthesis, and Biological Evaluation of New Tubulysins With Highly Potent Cytotoxicities Against Cancer Cells as

Potential Payloads for Antibody–Drug Conjugates," *Journal of the American Chemical Society* 140 (2018): 3690.

50. Z. Wang, P. A. McPherson, B. S. Raccor, et al., "Structure–Activity and High-Content Imaging Analyses of Novel Tubulysins," *Chemical Biology & Drug Design* 70 (2007): 75.

51. O. Pando, S. Stark, A. Denkert, et al., "The Multiple Multicomponent Approach to Natural Product Mimics: Tubugis, N-Substituted Anticancer Peptides With Picomolar Activity," *Journal of the American Chemical Society* 133 (2011): 7692.

52. A. Ullrich, Y. Chai, D. Pistorius, et al., "Pretubulysin, a Potent and Chemically Accessible Tubulysin Precursor From *Angiococcus Disciformis*," *Angewandte Chemie International Edition* 48 (2009): 4422.

53. J. Hoffmann, J. Gorges, L. Junk, and U. Kazmaier, "Synthesis of Pretubulysin Derivatives via the TubUgi Approach," *Organic & Biomolecular Chemistry* 13 (2015): 6010.

54. L. R. Staben, S.-F. Yu, J. Chen, et al., "Stabilizing a Tubulysin Antibody–Drug Conjugate to Enable Activity Against Multidrug-Resistant Tumors," *ACS Medicinal Chemistry Letters* 8 (2017): 1037.

55. W. Richter, "Tubulin Inhibitors," International Patent Application WO2011/057805A1, May 19, 2011.

56. J. L. Burkhart, R. Müller, and U. Kazmaier, "Syntheses and Evaluation of Simplified Pretubulysin Analogues," *European Journal of Organic Chemistry* 2011 (2011): 3050.

57. H. Van Le, L. Van Tran, A. T. Tran, et al., "Design, Synthesis, and Cytotoxic Activity of New Tubulysin Analogues," *Synlett* 33 (2022): 187.

58. M. Sani, G. Fossati, F. Huguenot, and M. Zanda, "Total Synthesis of Tubulysins U and V," *Angewandte Chemie International Edition* 46 (2007): 3526.

59. C. Schweigert, O. Babii, S. Afonin, et al., "Real-Time Observation of Diarylethene-Based Photoswitches in a Cyclic Peptide Environment," *ChemPhotoChem* 3 (2019): 403.

60. I. M. Welleman, M. W. Hoorens, B. L. Feringa, H. H. Boersma, and W. Szymański, "Photoresponsive Molecular Tools for Emerging Applications of Light in Medicine," *Chemical Science* 11 (2020): 11672.

61. S. H. Ibbotson, T. H. Wong, C. A. Morton, et al., "Adverse Effects of Topical Photodynamic Therapy: A Consensus Review and Approach to Management," *British Journal of Dermatology* 180 (2019): 715.

62. A. E. Prota, K. Bargsten, D. Zurwerra, et al., "Molecular Mechanism of Action of Microtubule-Stabilizing Anticancer Agents," *Science* 339 (2013): 587.

63. A. E. Prota, M. M. Magiera, M. Kuijpers, et al., "Structural Basis of Tubulin Tyrosination by Tubulin Tyrosine Ligase," *Journal of Cell Biology* 200 (2013): 259.

64. A. B. Waight, K. Bargsten, S. Doronina, M. O. Steinmetz, D. Sussman, and A. E. Prota, "Structural Basis of Microtubule Destabilization by Potent Auristatin Anti-Mitotics," *PLoS One* 11 (2016): e0160890.

## Supporting Information

Additional supporting information can be found online in the Supporting Information section.